学号_____

年级_____

河海大学

本科毕业论文

结合高度计的 UWB 的空间定位技术与应用

专　　业　电子信息工程

姓　　名　杨晟

指导教师　李东新 教授

评 阅 人_____

2019 年 5 月

中国　南京

BACHELOR'S DEGREE THESIS
OF HOHAI UNIVERSITY

Positioning technology and application of UWB with altimeter

College ： College of Computer and Information

Subject ： Electronic Information Engineering

Name ： Sheng Yang

Directed by ： Dongxin Li Professor

NANJING CHINA

郑 重 声 明

本人呈交的毕业论文，是在导师的指导下，独立进行研究工作所取得的成果，所有数据、图片资料真实可靠。尽我所知，除文中已经注明引用的内容外，本设计（论文）的研究成果不包含他人享有著作权的内容。对本设计（论文）所涉及的研究工作做出贡献的其他个人和集体，均已在文中以明确的方式标明。本设计（论文）的知识产权归属于培养单位。

本人签名：_____　　日期：_____

摘 要

无线通信正在成长为我们日常生活的重要组成部分。 卫星通信，蜂窝网络，无线局域网（WLAN）和无线传感器网络（WSN）是我们每天使用的这些无线技术。超宽带（UWB）是一种具有大带宽的有前途的技术。 UWB 的这种独特特性使其成为各种通信，测距和雷达的有吸引力的技术。 本文将重点关注基于 UWB 的精确定位方面。 由于锚的位置必须手动确认，这有点不方便并且可能带来巨大的错误。 因此，我使用高度计传感器来帮助定位所有锚点在 z 轴上的位置。 进行实验以比较使用高度计和不使用高度计的性能

关键词：无线网络；超宽带定位；定位技术；测高计

ABSTRACT

Wireless communications are growing up to be an essential part of our everyday lives. Satellite communications, cellular networks, wireless local area networks (WLANs), and wireless sensor networks (WSNs) are these wireless technologies that we use every day. Ultra-wideband (UWB) is a promising technology which has large bandwidths. Such unique trait of UWB turns it into an attractive technology for diverse communications, ranging, and radar. This paper would focus on the aspect of precise localization based on UWB. Since the positions of anchors must be confirmed manually, which is a little inconvenient and may bring enormous error. Therefore, I use the altimeter sensor to help locate all anchors& position in z-axis. An experiment is conducted to compare the performance of using altimeter and without it.

Key words: wireless networks；Ultra-wideband；localization； altimeter

Contents

Chapter 1 Introduction

1.1 Problem and Research Significance

As wireless devices are growing up to be more and more integrated into our everyday lives, they are also getting more and more intelligent. In the book[1], it says wireless devices are becoming more context aware, which is described as the ability of the mobile device to be aware of the its surrounding environment. Another definition means that if a system is context aware, it will offer relevant information and services to the user, which depends on the user's aims or tasks. Usually those services are based on the context information such as time, location, temperature, speed, orientation, biometrics, audio/video recordings, etc.

Among this various information above, location is the main focus in my paper and is probably the most prevalent factor which depicts a specific situation. For example in cellular system, location information can be utilized to Emergency services (911), resource management, and intelligent logistic systems. In hospitals location of the patients, injured tourists on mountains, or firefighters inside a building are some examples showing how location information work in an emergency circumstance. As an office worker, it would be convenient to find the closest printer while knowing your position in a wireless network. A customer can receive advertisements based on location in a supermarket. Such intelligent wireless network application with location information would make our live much comfortable and easier.

Real Time Location Systems (RTLS) describes a class of systems that provide information in real-time about the location of objects, animals, people or just about anything you care about. The most typical example of a RTLS is Global Positioning Systems (GPS) developed by the US Department

of Defense. It uses the time difference of arrival (TDOA) information from four or more of 24 satellites around the world to estimate target's outdoor position with an accuracy between 1 and 5 m; but it performs poorly for the indoors environment since walls block GPS signals. Indoor localization system may need other technology to locate target.

In general, there exists four fundamental signaling scheme that can be used for a localization system. Radio frequency (RF) maybe the most commonly used signaling scheme for localization purposes since RF signals can penetrate through obstacles and propagate to long distances. Cheng Chen[2] employed Wi-Fi, odometer and IMU (Inertial measurement unit) fusion for indoor positioning, and get good results. Infrared signals are low power consuming and cheap; however, they cannot penetrate through obstructions (contrast to RF), and are vulnerable against sunlight. Optical signals also require line-of-sight (LOS) conditions, affected by sunlight, but are low power consuming. They provide high accuracy and are normally more appropriate for short ranges (like about 10 m). Liu's Research[3] achieved sub-meter accuracy with fluorescent light communication system. Finally, an inexpensive signaling scheme is ultrasound signals, which have high accuracy in the short range. An advantage of acoustic signals is that the sound travels slowly. Therefore, the localization system doesn't require high clocks to timestamp messages, and can be achieved inexpensively in LOS conditions. With acoustic sensors Qiu[4] also realize a sub-meter localization system. However, ultrasound signals cannot work well in non-line-of-sight (NLOS) scenario.

Ultra-Wideband (UWB) is a RF technology which can achieve centimeter-level positioning and a range of up to 300 meters. Many researches have been done using UWB technology, such as Tiemann's Unmanned Aerial Vehicle (UAV) navigation[5] and Shi's formation flight system[6], and they all get great results. My research would also base on RF signals with

UWB technology to achieve a RTLS.

There are numerous properties of radio waves used to achieve radio positioning. For instance, time-of-arrival (TOA), time difference of arrival (TDOA), angle of arrival (AOA), and received signal strength (RSS). Various methods have been developed over these years to measure radio waves like time-of-flight (TOF), signal phase, signal strength and angle of arrival. In most cases, the localization system based on determining the TOF, which is a similar concept of the TOA, can realize high accuracy. A fundamental localization method is trilateration. In this case, at least three serving reference node (RN) are required for two-dimensional (2-D) localization, and at least four RNs are required for three-dimensional (3-D) localization. In a localization system, the communication node is often classified as mobile station and base station. Moreover, mobile station may equal to tag and base station is often referred to as anchor. In the case of trilateration, if the absolute location of the anchors is known in 2D or 3D space then the absolute location of the tags is also known. Thus, measuring the absolute location of the anchors improperly may bring enormous error. This paper uses the altimeter sensor to help mitigate all anchors& position error in z-axis.

1.2 Main Design of This System

UWB is an excellent RF technology for high accuracy localization in short (less than 100 m) to medium (up to 2000 m) distances due to its high time resolution and inexpensive circuitry. There are already a number of UWB ranging and positioning devices in the market. Being compliant with IEEE802.15.4 standard, the Sapphire DART system from Multispectral Solutions, Inc, Ubisense real-time location system and DecaWave's DW1000[7] are all available UWB localization products. An ideal localization system should fit in all kinds of application, such as accuracy, cost, range, and complexity. In order to reach these goals, a positioning node is designed

with DecaWave’s DWM1000 module[8].

Many RTLS based on UWB technology like Tiemann’s and Shi’s need to calculate or confirm all anchors’ absolute position manually, which usually results in each anchor mounts on a regular shelf or framework (like cuboid and so on). But when employing their system into a more bigger space, it might become inappropriate as well as deteriorate its accuracy. To mitigate this drawback, a compensation approach is present and will be evaluated by taking advantage of altimeter.

Chapter 2 System Theory Analysis

2.1 Ultra-Wideband

Guglielmo Marconi's spark gap radio transmitters send UWB signals across the Atlantic Ocean in 1901, but the precise investigation of UWB systems was conducted by the studies on impulse response characterization of microwave networks in the 1960s. Early names of UWB technology include baseband, carrier-free, non-sinusoidal and impulse. The US Department of Defense named the term UWB in the late 1980s. A UWB signal is characterized by its very large bandwidth compared to the conventional narrowband systems, which means a signal is called UWB if it has an absolute bandwidth of at least $500\ \text{MHz}$, or its fractional bandwidth is larger than 0.2. The absolute bandwidth is calculated as the difference between the upper frequency f_H of the $-10\ \text{dB}$ emission point and the lower frequency f_L of the $-10\ \text{dB}$ emission point:

$$B = f_H - f_L \tag{2.1}$$

which is also called $-10\ \text{dB}$ bandwidth. Besides, the fractional bandwidth is defined as

$$B_{\text{frac}} = \frac{B}{f_c} \tag{2.2}$$

where f_c is the center frequency and is given by

$$f_c = \frac{f_H + f_L}{2} \tag{2.3}$$

the fractional bandwidth B_{frac} in (2.2) can be written as from (2.1) and (2.3)

$$B_{\text{frac}} = \frac{2(f_H - f_L)}{f_H + f_L} \tag{2.4}$$

In accordance with the definition of the US FCC[9], a UWB system with f_c that is larger than $2.5\ \text{GHz}$ must have an absolute bandwidth larger than 500

MHz, and then a UWB system with f_c which is less than 2.5 GHz must have a fractional bandwidth larger than 0.2 as showing in Fig. 2.1

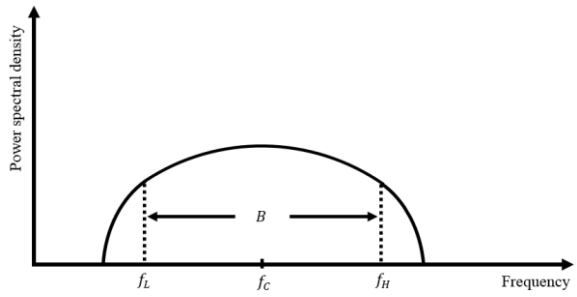

Fig. 2. 1 A UWB signal have an absolute bandwidth $B \geq 500\,MHz$ or a fractional bandwidth $B_{frac} > 0.2$

Because of its large bandwidth, the UWB system has very short duration waveforms, which usually is several nanoseconds. Ordinarily, the UWB system transmits ultra-short pulses with a low duty cycle. In this case, the ratio between the pulse transmission moment and the average time between two consecutive transmission frames is normally kept small, which commonly bring an advantage that saving power and energy. Nevertheless, it is reasonable to keep both low duty cycle instant and continuous transmission frames.

In a UWB system, numerous pulses are transmitted per information symbol and information is usually transferred by the positions or the polarities of the pulses, which was shown in Fig. 2.2. Each pulse occupies in an interval called a "frame", and the positions of the pulses in the frames are determined by a time-hopping (TH) code so that reduce the probability of collisions with pulses from other UWM system. In Fig. 2.2, three information have been transmitted, and each bit is composed of two pulses or two frames. The TH code of the first bit is {2,1}, which implied that in the first frame the pulse is shifted by $2T_c$ seconds and the second one is shifted by T_c seconds, where T_c refers to the chip interval.

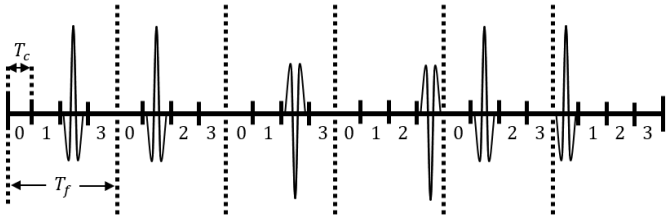

Fig. 2. 2 A UWB signal whose positions of the pulses in different frames are determined by a TH code, which is $\{2,1,2,3,1,0\}$ in this example

2.2 Basic Positioning Methods

There are a variety of different methods of position determination in RTLS using radio signals but they effectively devolve into two basic types of scheme:

1) Those based on radio signal strength - commonly referred to as Received Signal Strength Indication (RSSI/RSS) scheme;

2) Those based on the Time of flight - where the time the radio signal takes traveling between transmitter and receiver is measured and the distance can be calculated by using the speed of light. For example, Time of Arrival, Time Difference of Arrival and Phase difference of Arrival (PDOA) are three main methods based on Time of flight.

2.2.1 Received signal strength

In this situation, we need to measure the signal strength of the arriving radio signal at the receiver. Given the power at which the signal was transmitted from the transmitter, the propagation characteristics of this radio signal in air and with some a preferred knowledge of the environment, then it is possible to calculate approximately where the transmission derived based on how attenuated it is at the receiver.

However, since the RSS usually has a specific (static) distribution pattern over the localization area, if other objects enter or move in that area (like people or animals) the distribution pattern would change perceptibly. This change may greatly worsen the reliability of the localization system.

On the other hand, such characteristic also has some advantages. In the field of detection for intrusions or burglaries, positioning needs to be achieved without performing any communications between the target (intruder) and the base stations. Using the RSS method and analyzing for any change in an otherwise static signal pattern, possible intrusions can be detected.

2.2.2 Time of Arrival

Working on the basis of determining the time it spends for a radio signal on transmitting from a transmitter to a receiver, the distance between the transmitter and the receiver can be determined as long as this time is calculated precisely, given that the speed of propagation of radio waves in air is known.

Applying the Time of Arrival method to achieve a RTLS, the distance between the tags and several anchors in known locations must be measured. In Fig. 2.3 we can see that anchor $P1$ measures the distance between itself and the tag B as $r1$. This locates the tag B on a circle of radius $r1$ from the anchor $P1$. It is the same case that $P2$ measures the distance with the tag B as $r2$ and $P3$ gets the distance as $r3$. According to a fundamental localization method, which is trilateration, calculating the point of intersection between these three circles could figure out the position of tag B. The prior condition of this method is the absolute location of the anchors required to be known.

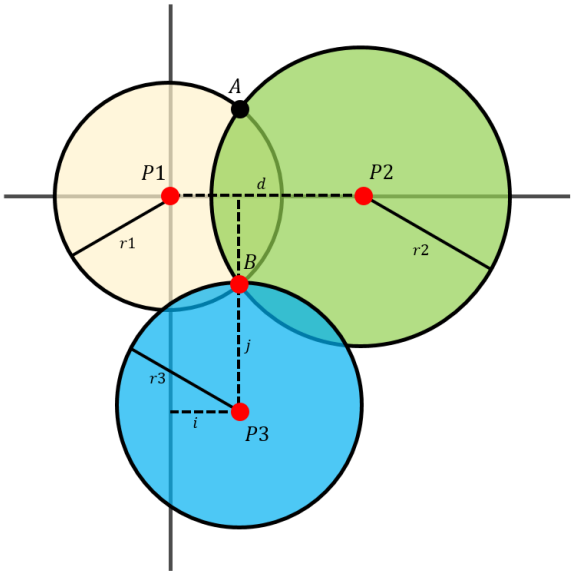

Fig. 2. 3 Time of Arrival method

2.2.3 Time Difference of Arrival

The similar requirement of TDOA as TOA is that three or more anchors are utilised in known locations in the environment to locate the positions of the tags. But each of these anchors is time synchronized to the others.

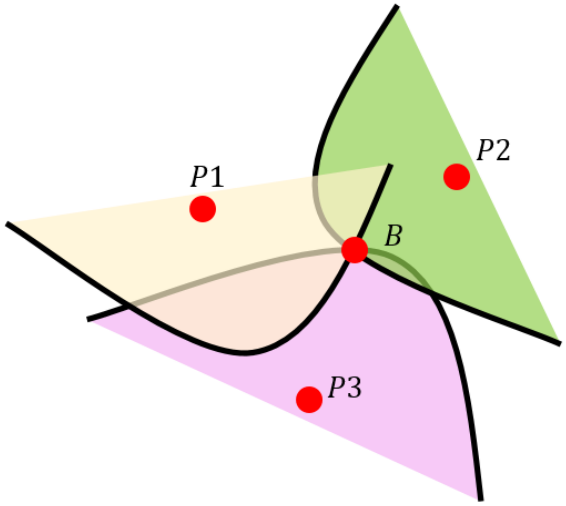

Fig. 2. 4 Time Difference of Arrival method

As shown in Fig. 2.4 the tag B transmits a message that is received by all the anchors ($P1, P2$ and $P3$). Due to radio wave propagates in air at a constant speed, relying on the position of the tag B, the message will reach at some of the anchors before others. Each anchor will record the time of arrive of this message. Because all three anchors are time synchronized,

the difference of the time of arrive among all anchors could estimate the position of the tag B.

Obviously, the most difficult issue in this method is how to synchronize all anchors in time. Any error produced in the synchronization process will directly affect the accuracy of this RTLS. It is because a UWB pulse duration is usually less than $1\ \text{ns}$, you can think that $1\ \text{ns} = 30\ \text{cm}$, which means that the synchronization error must to be controlled within the sub-nanosecond level to realize high accuracy.

2.2.4 Phase Difference of Arrival

The conception of Phase Difference of Arrival is to calculate the distance between an anchor and a tag as well as the x,y location of this tag relative to the corresponding anchor.

This method generally uses an array of antennas in the anchor. The time of arrive at different antennas will be measured and then the difference for all TOAs is compared. Showing in Fig. 2.5.

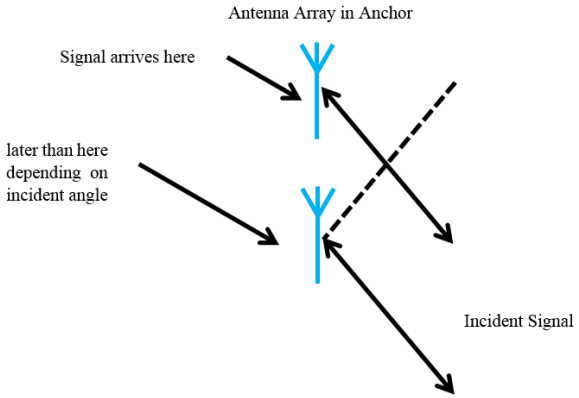

Fig. 2. 5 Phase Difference of Arrival antenna array

If the tag is coincidentally perpendicular to the antennas in the array, the incident signal would arrive at all the antennas at the same time, so there would be no difference in TOA. In most cases, the tag is at some angle to the array so that the incident signal will arrive at one antenna in the array first and then next one and so on. It is possible to derive the location of this tag with precise measurement of Phase Difference of Arrival. On

the other hand, increasing the number of antennas per anchor would apparently adds cost to the RSTL.

2.3 Position Determination Algorithm

Most of common position determination algorithms are based on the measurement of the TOA of the radio signal, since it can provide the most accurate position determination. Due to this measurement is the arrival time at the receiver rather than the Time of Flight, the available measurement data are pseudo-ranges (range plus an unknown offset), compared to ranges, there are a number of position determination algorithms used to process these pseudo-ranges data in a classical localization system where several fixed anchors are used to determine the location of a tag.

2.3.1 Noniterative Position Determination

Focusing on noniterative position determination methods, the raw measured data are processed using analytical formulas to calculate the position of a tag directly. Such algorithms are trilateration, spherical interpolation (SI), quasi-least squares (QLS), and linear correction least-squares (LC-LS). Although these methods can definitely get a position fix, the analytical equations would be computationally intensive. Thus they might not be appropriate for simple localization system with several nodes and limited computational capability.

1) Trilateration Position Calculation

In Fig. 2.3 showing a simple example of how to calculate the location of the tag with the distance measurements from three anchors in a 2D environment. The tag can communicate with three anchors and its position is located on each distance circle with the corresponding anchor location as the center and the distance as the radius. Generally, two distance circles intersect at two points, which would produce two solutions for the position estimate of the tag. Therefore, a third anchor is needed to produce a third distance circle in order to solve this ambiguity of the two solutions.

In general, these circles will not intercross at one point, thus, other methods are required to calculate the position. There is a straightforward way that to compute the distance between the third anchor and each of the two solutions. The two result distances are then compared with the third distance circle each other. The one which better matches with third anchor will be the solution, which can be seen that the tag and three anchors cannot lie in a straight line to calculate a unique position estimate. In Fig. 2.6, a 3D position estimation is shown.

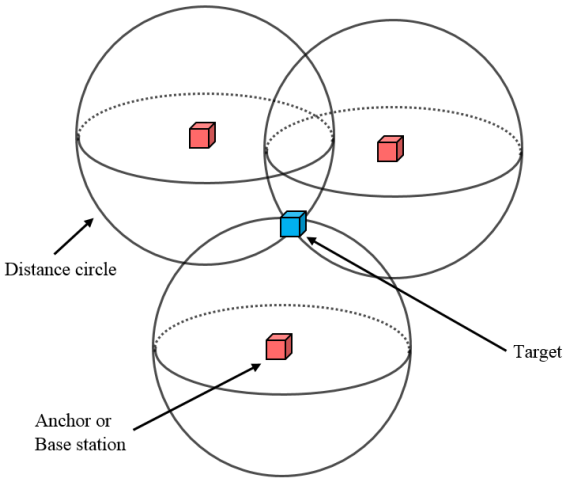

Fig. 2. 6 Position estimation in 3D environment

Suppose that there are four anchors with known locations given by $(x_i, y_i, z_i), 1 \leq i \leq 4$, and that the unknown location of the target is denoted by (x, y, z). The distance measurement equations are defined as

$$\hat{d}_i = d_i + \varepsilon_i \quad i = 1, 2, 3, 4 \tag{2.5}$$

where ε_i is the distance measurement error and

$$d_i = \sqrt{(x - x_i)^2 + (y - y_i)^2 + (z - z_i)^2} \tag{2.6}$$

Since there are three unknown location parameters, let us first use three distance measurements, say $\hat{d}_1, \hat{d}_2$ and $\hat{d}_3$, to determine the location. Define

$$\begin{aligned} \zeta_{i,1} &= x_i^2 + y_i^2 + z_i^2 - (x_1^2 + y_1^2 + z_1^2) \\ x_{i,j} &= x_i - x_j \\ y_{i,j} &= y_i - y_j \end{aligned} \tag{2.7}$$

$$z_{i,j} = z_i - z_j$$

$$f_{1,i} = \frac{1}{2}\left\{\left(\hat{d}_1{}^2 - \hat{d}_i{}^2\right) + \zeta_{i,1}\right\}$$

Also define

$$\begin{aligned}
\kappa_1 &= \frac{x_{2,1}z_{3,1} - x_{3,1}z_{2,1}}{x_{3,1}y_{2,1} - x_{2,1}y_{3,1}} \\
\kappa_2 &= \frac{x_{3,1}f_{1,2} - x_{2,1}f_{1,3}}{x_{3,1}y_{2,1} - x_{2,1}y_{3,1}} \\
\kappa_3 &= \frac{y_{3,1}z_{2,1} - y_{2,1}z_{3,1}}{x_{3,1}y_{2,1} - x_{2,1}y_{3,1}} \\
\kappa_4 &= \frac{y_{2,1}f_{1,3} - y_{3,1}f_{1,2}}{x_{3,1}y_{2,1} - x_{2,1}y_{3,1}}
\end{aligned} \tag{2.8}$$

Then, with some mathematical manipulations, it can be shown that the estimate of the z-coordinate of the position is

$$\hat{z} = \frac{h_2}{h_1} \pm \sqrt{\left(\frac{h_2}{h_1}\right)^2 - \frac{h_3}{h_1}} \tag{2.9}$$

Where

$$\begin{aligned}
h_1 &= \kappa_1^2 + \kappa_3^2 + 1 \\
h_2 &= \kappa_1(y_1 - \kappa_2) + \kappa_3(x_1 - \kappa_4) + z_1 \\
h_3 &= (x_1 - \kappa_4)^2 + (y_1 - \kappa_2)^2 + z_1^2 - \hat{d}_1^2
\end{aligned} \tag{2.10}$$

Accordingly, the estimates of the x-coordinate and y-coordinate can be obtained as

$$\begin{aligned}
\hat{x} &= \kappa_3\hat{z} + \kappa_4 \\
\hat{y} &= \kappa_1\hat{z} + \kappa_2
\end{aligned} \tag{2.11}$$

Clearly, there are two solutions, but only one of them is the desired one. The ambiguity can be resolved by making use of the measurement at the fourth anchor. Specifically, the residuals of the two location estimation solutions are calculated by

$$\begin{aligned}
v_1 &= \left[\sqrt{(x_4 - \hat{x}^{(1)})^2 + (y_4 - \hat{y}^{(1)})^2(z_4 - \hat{z}^{(1)})^2} - \hat{d}_4\right]^2 \\
v_2 &= \left[\sqrt{(x_4 - \hat{x}^{(2)})^2 + (y_4 - \hat{y}^{(2)})^2(z_4 - \hat{z}^{(2)})^2} - \hat{d}_4\right]^2
\end{aligned} \tag{2.12}$$

If $v_1 > v_2$, then the second solution $(\hat{x}^{(2)}, \hat{y}^{(2)}, \hat{z}^{(2)})$ is chosen. Otherwise, the first solution $(\hat{x}^{(1)}, \hat{y}^{(1)}, \hat{z}^{(1)})$ is selected. To make the residual-based judgment as reliable as possible, the fourth anchor should not be on the same plane formed by the other three anchors.

2) Least-Squares Method based on an Intermediate Variable

When the system is overdetermined, which means the number of independent equations is greater than the number of unknown parameters, the Least-Squares (LS) method can be applied to make use of the redundant measurements to obtain improved location estimates.

Consider a network in which there are N anchors whose locations are known and denoted by $(x_i, y_i, z_i), i = 1, 2, \cdots, N$. The unknown location of the target is defined as (x, y, z). When a distance measurement is made at each anchor, there are N measurement equations:

$$\hat{d}_i = d_i + v_i \quad i = 1, 2, \cdots, N \tag{2.13}$$

Where

$$d_i = \sqrt{(x_i - x)^2 + (y_i - y)^2 + (z_i - z)^2} \tag{2.14}$$

and v_i is the measurement error.

Linearization of the distance measurement equations can be realized by introducing a new variable. Specifically, squaring both sides of (2.13) produces

$$-(2x_i x + 2y_i y + 2z_i z) + (x^2 + y^2 + z^2) = \left(\hat{d}_i - v_i\right)^2 - \left(x_i^2 + y_i^2 + z_i^2\right) \tag{2.15}$$

Then, by defining

$$\begin{aligned} R &= \sqrt{x^2 + y^2 + z^2} \\ R_i &= \sqrt{x_i^2 + y_i^2 + z_i^2} \end{aligned} \tag{2.16}$$

(2.15) becomes

$$-(2x_i x + 2y_i y + 2z_i z) + R^2 = \hat{d}_i^2 - R_i^2 + v_i^2 - 2\hat{d}_i v_i \tag{2.17}$$

which can be written in a compact form as

$$\mathbf{h} = \mathbf{G}\theta + \mathbf{v} \tag{2.18}$$

Where

$$\begin{gathered}\theta = [x \quad y \quad z \quad R^2]^{\mathrm{T}} \\ \mathbf{h} = \begin{bmatrix} \hat{d}_1^2 - R_1^2 \\ \hat{d}_2^2 - R_2^2 \\ \vdots \\ \hat{d}_N^2 - R_N^2 \end{bmatrix} \\ \mathbf{G} = \begin{bmatrix} -2x_1 & -2y_1 & -2z_1 & 1 \\ -2x_2 & -2y_2 & -2z_2 & 1 \\ \vdots & \vdots & \vdots & \vdots \\ -2x_N & -2y_N & -2z_N & 1 \end{bmatrix} \\ \mathbf{v} = [-v_1^2 + 2\hat{d}_1 v_1 \quad -v_2^2 + 2\hat{d}_2 v_2 \quad \cdots \quad -v_N^2 + 2\hat{d}_N v_N]^{\mathrm{T}}\end{gathered} \tag{2.19}$$

The LS solution of (2.18) is

$$\hat{\theta} = (\mathbf{G}^{\mathrm{T}}\mathbf{W}\mathbf{G})^{-1}\mathbf{G}^{\mathrm{T}}\mathbf{W}\mathbf{h} \tag{2.20}$$

where $\mathbf{W} = \mathrm{cov}^{-1}(\mathbf{v})$ is the weighting matrix which is set to be the inverse of the covariance matrix of $\mathbf{v}$ for Gaussian noise. In the case of unknown statistics of the error vector $\mathbf{v}$, $\mathbf{W}$ may be set at a diagonal matrix with the SNRs determined by receivers as the diagonal elements, or simply set at an identity matrix.

2.3.2 Iterative Position Determination

In this case, iterative methods are used to solve the nonlinear equations which describe the position determination problem. For example, there are Taylor series least squares (TS-LS) method, the iterative optimization method and the maximum likelihood (ML) method and Kalman filter iterative method. Commonly, these iterative methods need an initial 'guess' of the position, but in some situation, especially when large measurement errors are present these algorithms may not converge. Nevertheless, in the localization system while continuous periodic updates are running, the previous position can be used as the initial position,

which normally approaches to a rapid convergence of position determination without large computation contrasting to the noniterative methods.

2.4 Indoor Height Determination

In order to measure the height between the target object and reference plain, there are several kinds of commercial sensors could be used. They may be classified as three types: laser, ultrasonic and barometer. The first two types both can achieve high accuracy and stability, but they all need the line of sight environment, which means that if height measurement is required, these sensors must be installed on the bottom of the target object and should be toward to the reference plain (like ground), and the line between them cannot be block by other obstacles. As a result, it is inconvenient to utilize the laser or ultrasonic sensors to measure height. However, the barometer (or altimeter) can determine the height without the line of sight requirement.

2.4.1 Atmospheric pressure measurement

The atmospheric pressure is the weight exerted by the overhead atmosphere on a unit area of surface. It can be measured with a mercury barometer, as shown in Fig.2.7.

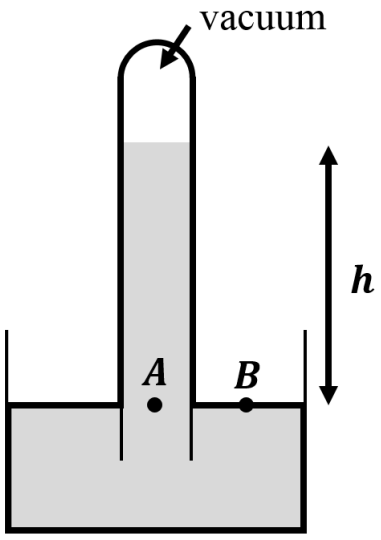

Fig. 2. 7 Mercury barometer

There is a long glass tube that is full of mercury inverted over a pool of mercury. According to some physical knowledge, it is well known that the pressure P_A at point A is equal to the pressure P_B at point B and the equilibrium equation can be represented as:

$$P_A = \rho_{Hg}\, gh \tag{2.21}$$

where $\rho_{Hg} = 13.6\,\mathrm{g\,cm^{-3}}$ is the density of mercury and $g = 9.8\,\mathrm{m\,s^{-2}}$ is the acceleration of gravity. The mean value of h measured at sea level is $76.0\,\mathrm{cm}$, hence, the corresponding atmospheric pressure is $1.013 \times 10^5\,\mathrm{kg\ m^{-1}\ s^{-2}}$; $1\,\mathrm{Pa} = 1\,\mathrm{kg\ m^{-1}\ s^{-2}}$. There are also some customary pressure such as the atmosphere (atm) ($1\,\mathrm{atm} = 1.013 \times 10^5\,\mathrm{Pa}$), the bar (b) ($1\,\mathrm{b} = 1 \times 10^5\,\mathrm{Pa}$), the millibar (mb) ($1\,\mathrm{mb} = 100\,\mathrm{Pa}$), the torr $1\,\mathrm{torr} = 1\,\mathrm{mm\ Hg} = 134\,\mathrm{Pa}$) and the hectoPascals (hPa). The mean atmospheric pressure at sea level is given equivalently as $P = 1.013 \times 10^5\,\mathrm{Pa} = 1013\,\mathrm{hPa} = 1013\,\mathrm{mb} = 1\,\mathrm{atm} = 760\,\mathrm{torr}.$

2.4.2 Barometric law

Here the vertical profile of pressure will be explained. An elementary slab of atmosphere at altitude z with thickness dz, horizontal area A is shown in Fig. 2.8:

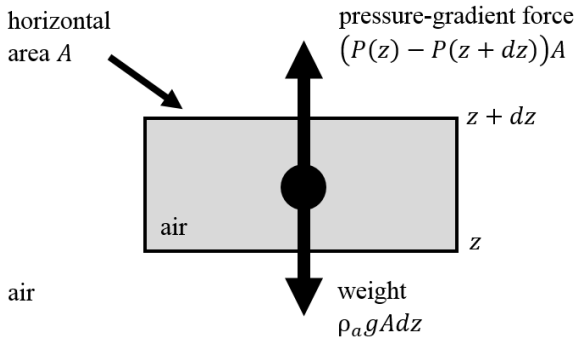

Fig. 2. 8 Vertical forces acting on an elementary slab of atmosphere

The outer atmosphere exerts an upward pressure force $P(z)A$ on the bottom of the slab and a downward pressure force $P(z+dz)A$ on the top of the slab. So the resultant force on the black net is $\big(P(z) - P(z+dz)\big)A$, which is also called the pressure-gradient force. Since $P(z) > P(z+dz)$, the

pressure-gradient force is directed upwards. In order to become equilibrium for the slab, its weight should equal to the pressure-gradient force:

$$\rho_a g A dz = \big(P(z) - P(z+dz)\big)A \tag{2.22}$$

rearranging and dP/dz can be seen:

$$\frac{dP}{dz} = \frac{P(z+dz) - P(z)}{dz} = -\rho_a g \tag{2.23}$$

since the ideal gas law is

$$\rho_a = \frac{PM_a}{RT} \tag{2.24}$$

where M_a is the molecular weight of air (common value is $28.96 \times 10^{-3}\,\mathrm{kg\,mol^{-1}}$), $R = 8.31\,\mathrm{J\,mol^{-1}\,K^{-1}}$ is the gas constant and T is the temperature (the unit usually is K). Substituting (2.24) into (2.23) produce:

$$\frac{dP}{P} = -\frac{M_a g}{RT} dz \tag{2.25}$$

Now if only the constant T with altitude situation is considered, using integration can yield:

$$P(z) = P(0)\exp\left(-\frac{M_a g}{RT} z\right) \tag{2.26}$$

equation (2.26) is called the barometric law[10]. Commonly a definition of the scale height H is used for the atmosphere:

$$H = \frac{RT}{M_a g} \tag{2.27}$$

producing a compact form for the barometric law:

$$P(z) = P(0)e^{-\frac{z}{H}} \tag{2.28}$$

However, the temperature will change according to altitude. The International Civil Aviation Organization (ICAO) defined the International Standard Atmosphere[11], which model the temperature variation as shown in Fig. 2.9:

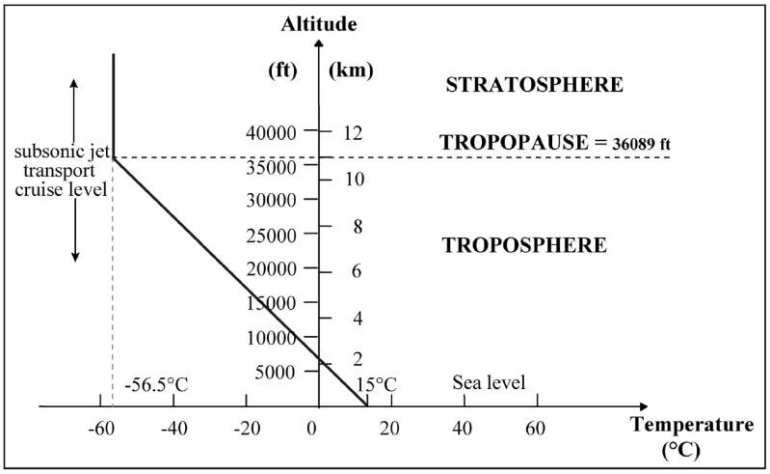

Fig. 2. 9 International Standard Atmosphere temperature variation

For example, in the troposphere (from $0\,\mathrm{m}$ to $11{,}000\,\mathrm{m}$) the temperature decreases with altitude at a constant rate of $-6.5℃/1000\mathrm{m}\,(-1.98℃/1000\mathrm{ft})$. So the ISA model presents the following characteristics within the troposphere:

$$T = T_0 - 6.5\frac{h - h_0}{1000} \tag{2.29}$$

where the unit of T and T_0 is K, and h and h_0 is in meters, and T_0 or h_0 could be the corresponding value at sea level.

Now replacing (2.29) into (2.25) and integrating both sides:

$$\int_{p_0}^{p}\frac{dp}{p} = -\frac{M_a g}{R}\int_{h_0=0}^{h}\frac{dh}{T_0 - 0.0065(h - h_0)} \tag{2.30}$$

performing the above integration, a simple formula can be produced:

$$p = p_0\left(1 - 0.0065\frac{h - h_0}{T_0}\right)^{5.2561} \tag{2.31}$$

2.4.3 Height measurement

It is well known that based on above law, in aircrafts altimeters use barometer to measure the air pressure and use this information to produce the altitude. Due to the real atmosphere never keep constant at any specific place or time, height measurement also need local air pressure information from such meteorological stations, airports or control towers as reference

points, and these reference stations should not be too far away from the interesting atmosphere environment[12].

To calculate height, the (2.31) of barometric law needs to be inverted as:

$$h = h_0 + \frac{T_0}{0.0065} - \frac{T_0}{0.0065}\left(\frac{p}{p_0}\right)^{\frac{1}{5.2561}} \tag{2.32}$$

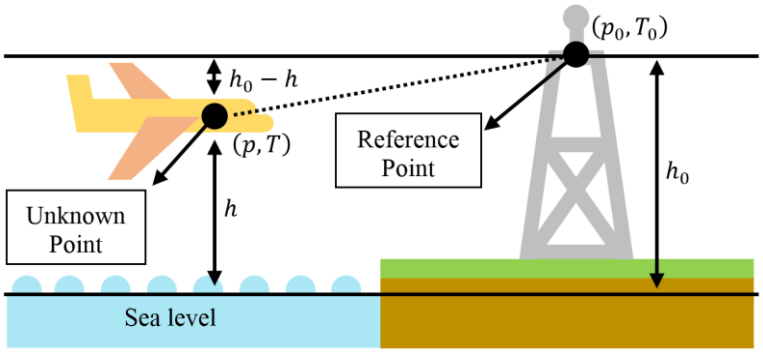

Fig. 2. 10 Height measurement from air pressure

As shown in Fig. 2.10, or referring to this paper[13], if the status (p_0, T_0, h_0) of the reference point is known and air pressure (p) is also known, it is possible to calculate the height (h) from equation (2.32) and relative height $(h - h_0)$.

Chapter 3 System Hardware Design

3.1 UWB localization module

The hardware design of the UWB localization module is presented in this chapter. As depicted in Fig.2.11, the whole module layout can be divided as six blocks: main controller, power, UWB module, sensors, button and led circuitry.

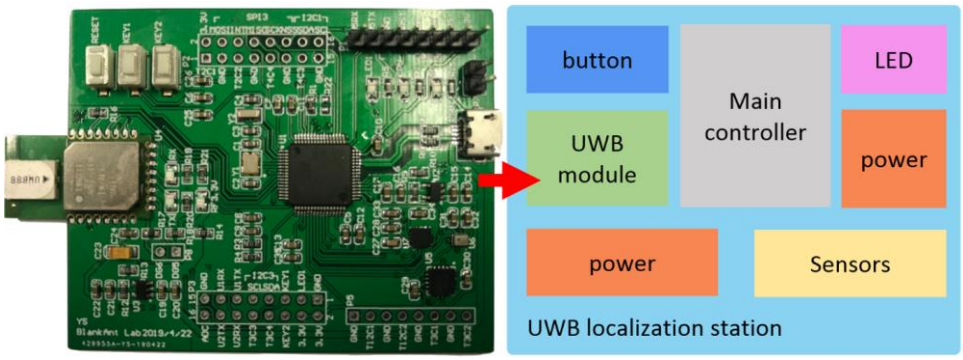

Fig. 2. 11 UWB localization module layout

3.1.1 Main controller

Considering the calculation performance, volume size and cost, the STM32F446xx microcontroller of the st company[14] has been chosen as the main controller for the UWB localization module. The STM32F446xx microcontroller is based on the ARM 32-bit Cortex-M4 CPU and its frequency can be up to 180 MHz with 225 DMIPS (Dhrystone Million Instructions executed Per Second). It also has a 512 kB flash memory and a 128 kB SRAM, which is suitable for its application.

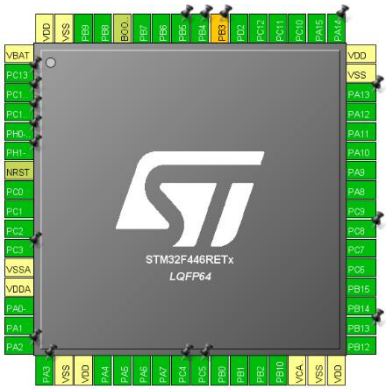

Fig. 2. 12 STM32F446xx microcontroller

3.1.2 Power design

According to the dw1000 hardware design guide[15], which could be as a reference sheet for the UWB module, two kinds of power circuitry has been designed and they are digital and RF management circuit separately in order to keep each of their noise away from itself. This power architecture can make sure that the UWB module and all sensors work steadily.

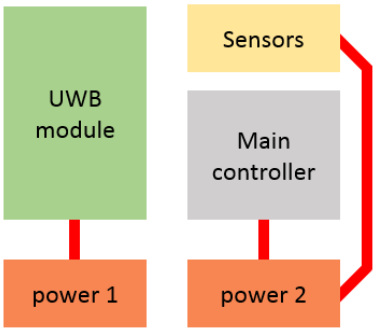

Fig. 2. 13 Power design

3.1.3 UWB module

There are various UWB products which are compliant with the IEEE802.15.4 standard. The DWM1000 module of the decaWave company is selected as the UWB module. It has many advantages for this research, such as high precision (about 10 cm indoors), allowing high data rate (up to 6.8 Mb/s), good communication range (maximum is 300 m), low power consumption (max working current is about 250 mA) and so on. A key trait is that its integrated antenna allows simple product implementation, therefore there is no RF design requirement for the research.

Fig. 2. 14 DWM1000 module

3.1.4 Altimeter

As for the altimeter, the SPL06-001 of the GoerTek company is the sensor

for the research. The SPL06-001 is a digital barometric air pressure sensor with high accuracy ($\pm$ 0.006 hPa or $\pm$ 5 cm) and low power consumption (about 60 μA). Its pressure operating range is between maximum 1200 hPa and minimum 300 hPa and temperature range is from 85 ℃ to − 40℃ which is appropriate for indoor environment.

Fig. 2. 15 SPL06-001 barometer

Chapter 4 System Software Design

4.1 UWB localization system

The software design of the UWB localization module is presented in this chapter. Its whole structure is shown in Fig.2.12 where four main software blocks has been drawn. They are positioning algorithm, distance measurement, height measurement and UWB communication framework software blocks.

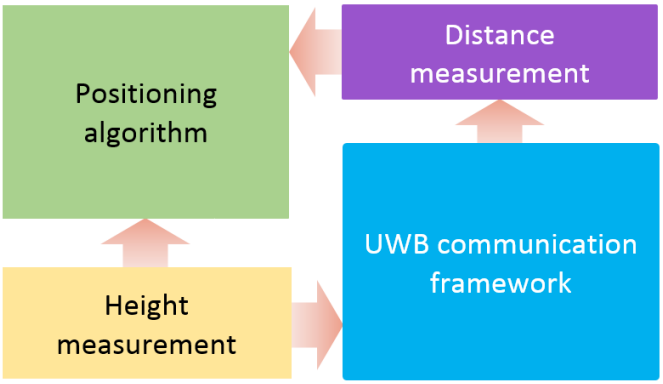

Fig. 2. 16 Software structure

4.1.1 Distance measurement method

This system employs two-way ranging exchange (TWR) to measure distance between the tag and each anchor, which is the unsynchronized positioning method in TOA. In this scene, the tag needs to communicate individually with each of all anchors and then each anchor will calculate the time of flight of the transmission from the tag. A simplified scheme of TWR is depicted in Fig.2.13 and can be described as below:

1) The tag transmits a message to an anchor and records the time t_1 when the message is emitted from its antenna;
2) The anchor receives the message and marks the time of arrive t_2;
3) The anchor sends back a reply and record the time t_3;
4) The tag receives the final message and marks the final time of arrive t_4;
5) Then the tag can calculate the distance between them since the speed of transmission is known.

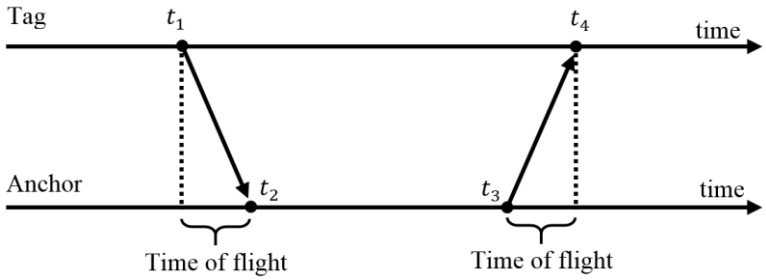

Therefore, according to the formula:

$$T_{\text{time of flight}} = \frac{t_2 - t_1 + t_4 - t_3}{2} \tag{2.33}$$

The distance between the tag and anchor can be solved. However, there are various physical effects such as clock drift which this simple scheme of TWR may be suffered greatly. Other more advanced scheme such as double-sided two-way ranging (DS-TWR) could use to correct these errors. A simplified double-sided two-way ranging is as shown in Fig. 2.13.

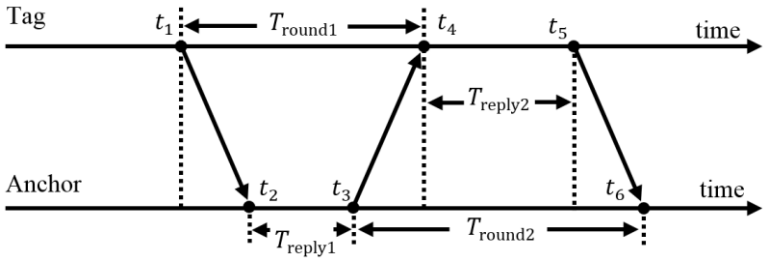

The resultant time of flight may be calculated by using the expression:

$$T_{\text{time of flight}} = \frac{\left(\mathrm{T_{round1}} \times \mathrm{T_{round2}} - \mathrm{T_{reply1}} \times \mathrm{T_{reply2}}\right)}{\left(\mathrm{T_{round1}} + \mathrm{T_{round2}} + \mathrm{T_{reply1}} + \mathrm{T_{reply2}}\right)} \tag{2.34}$$

In this method, the classic clock drift error is in the picosecond range even with 20 ppm crystals, and the major source of error is the precision of determining the arrival time of the messages at each of the receivers rather than the clock drift error.

4.1.2 UWB module communication framework

Using this UWB localization system, each of all five UWB localization modules has two mission. They are update height measurement and distance measurement respectively. As shown in Fig. 2.14, the first mission is that one of four anchors will act as a reference node to offer its own height, and remained anchors as well as the tag utilize this measurement as the

reference point to produce their own altitude. After finishing updating height measurement task, the tag would initiate the TWR exchange program to measure all distances between each four anchors and itself.

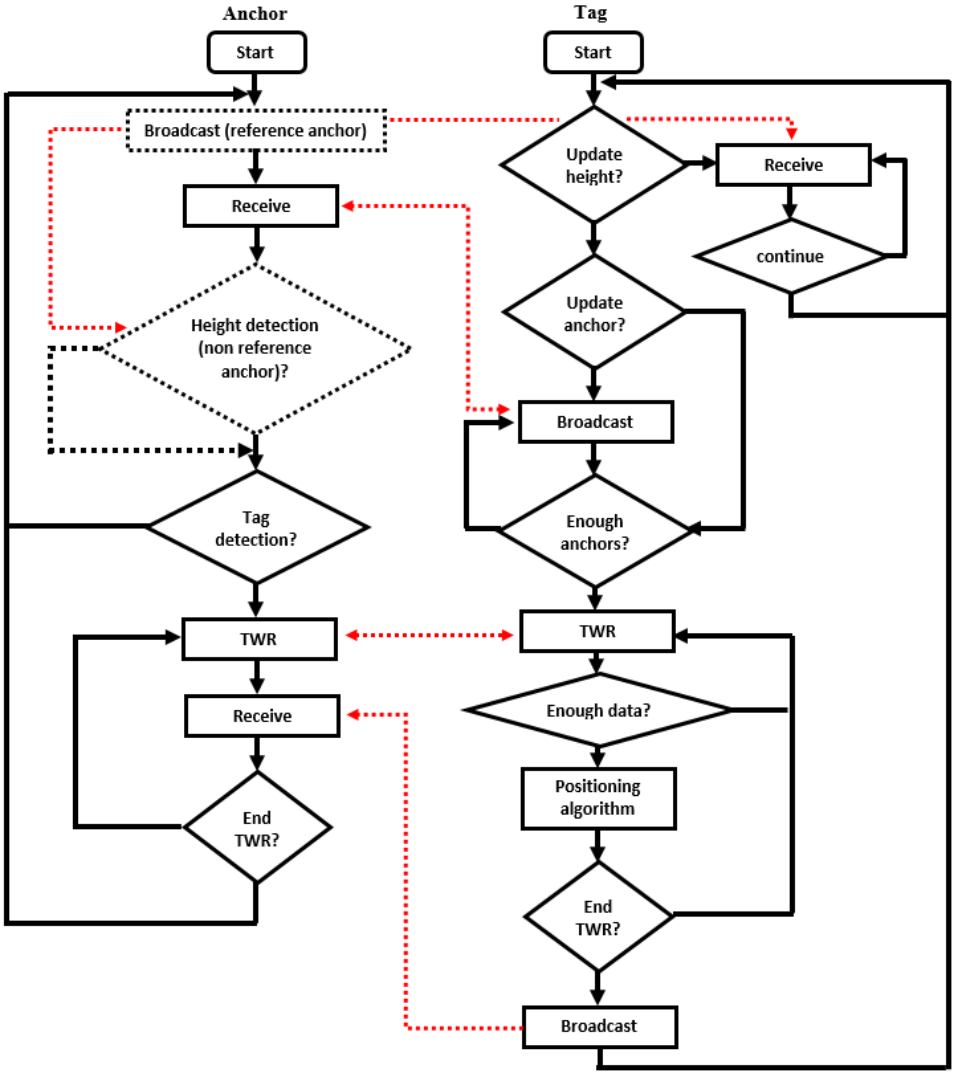

Fig. 2. 17 UWB module communication framework

1) Update height measurement task

In the first mission, one anchor operates as a reference point. Others units act as the receiver. The reference anchor broadcast the height measurement message and remainders wait to receive this message, which can be seen in Fig. 2.15. As for this research, all four anchors are named as Y_0, Y_1, Y_2, Y_3 and the tag is called the S_0. Then the Y_0 anchor is chosen for the reference point.

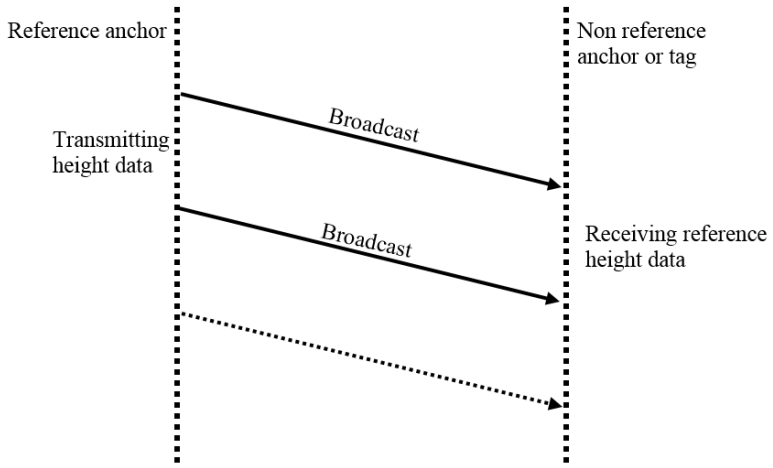

Fig. 2. 18 Update height measurement task

2) Distance measurement task

In two-way ranging exchange mission, two units exchange message with each other. But before starting this procedure, the unit as tag needs to inform all anchors in the UWB network to prepare themselves. This process is depicted in Fig.2.16:

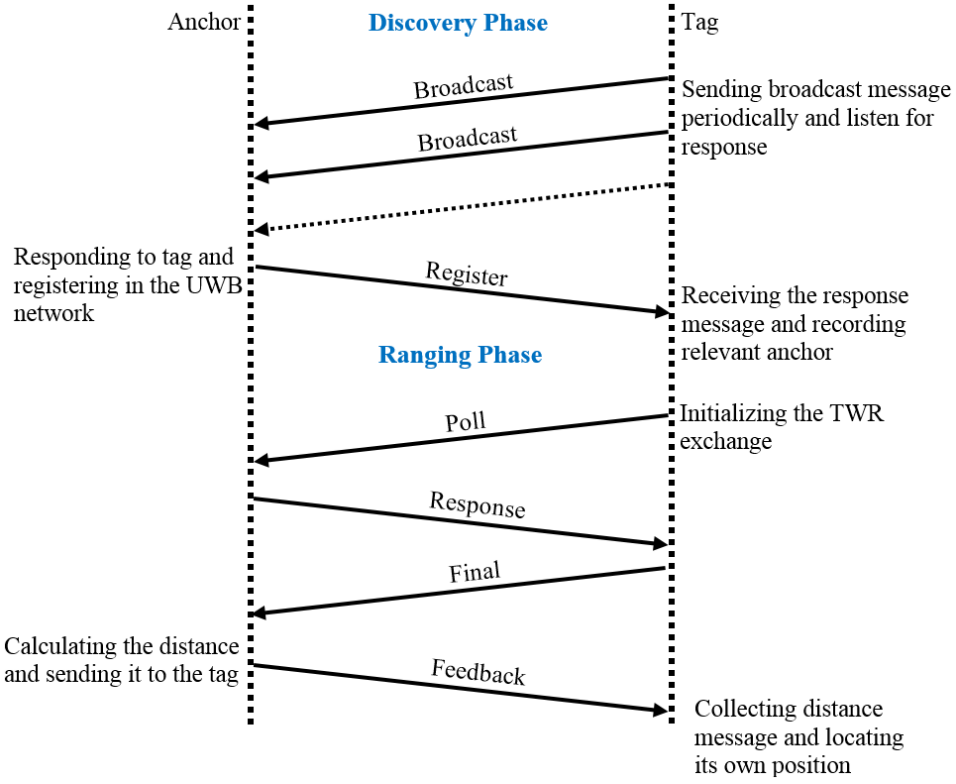

Fig. 2. 19 Distance measurement task

From the beginning of this task, the tag will send broadcast message

periodically and then listen for response from anchors, which is to make sure there would have enough data to calculate its position. After receiving the response of the anchor and obtaining enough number of registered anchors in the UWB network, the tag should initialize and perform the two-way ranging exchange until it acquires all the ranging data.

4.1.3 Altimeter height calculation

The barometer is the altimeter to measure the vertical distance between the anchors and reference plain. In general, many researches have been conducted to apply the barometer in indoor or outdoor environment. However, since the ambient air pressure measured are affected by the variation of surrounding temperature, ventilation and so on, the performance of the barometer usually is not ideal. Thus, the main error source of the barometer height must be researched. For most cases, it is composed of the bias term, drift term and noise term. The bias term, or initial sensor bias, normally is constant and could be removed by calibration. The drift term which is caused by the fluctuation of ambient temperature, ventilation and other uncertain factors. The noise term is the measurement noise of the barometric height. Hence, the height measurement of barometer can be represented as following:

$$\hat{P}_{\text{barometer}} = P_{\text{sea}} + \Delta P_{\text{barometer}} + P_{\text{bias}} + P_{\text{drift}} + n_{\text{barometer}} \tag{2.35}$$

where $\hat{P}_{\text{barometer}}$ is the measurement data from the barometer, and $\Delta P_{\text{barometer}}$ refers to the difference of the true pressure of current position of the barometer and the pressure in the sea level. In addition, $P_{\text{bias}}, P_{\text{drift}}$ and $n_{\text{barometer}}$ are individually the bias term, drift term and noise term talked above.

With the purpose of minimizing error from height measurement, the calibration algorithm and a second barometer as a reference point will be exercised. The solution is adjusting the barometer before using it for positioning as below:

1. Place the barometer and the reference one on the same horizontal plain and calculate the pressure offset ($\Delta\hat{P}^0_{\text{bias}} = \hat{P}^0_{\text{barometer}} - \hat{P}^0_{\text{reference}}$) between these two units;
2. Move these barometers to their targeted position and calculate their absolute height $h_{\text{barometer}} = h_0 + \frac{T_0}{0.0065} - \frac{T_0}{0.0065}\left(\frac{\hat{P}_{\text{barometer}} - \Delta\hat{P}^0_{\text{bias}}}{p_0}\right)^{\frac{1}{5.2561}}$ and $h_{\text{reference}} = h_0 + \frac{T_0}{0.0065} - \frac{T_0}{0.0065}\left(\frac{\hat{P}_{\text{reference}}}{p_0}\right)^{\frac{1}{5.2561}}$;
3. Compute the relative height $h_{\text{relative}} = h_{\text{barometer}} - h_{\text{reference}}$.

The reference point should not be too far away from the indoor environment where the barometer is installed since above formula requires a similar atmosphere.

4.1.4 Positioning algorithm design

Based on the trilateration positioning algorithm, the UWB localization system can locate the position of tag with the cooperation of four anchors. Working on the UWB module communication framework, the tag is able to exchange the ranging or broadcast messages orderly with all four anchors. As long as collecting enough ranging data, the tag will input these data to the trilateration positioning algorithm to locate its own position. The flow chart about it is drawn in Fig. 2.17.

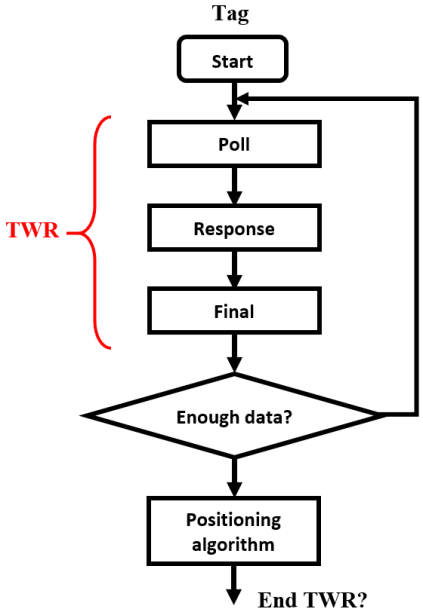

Fig. 2. 20 Positioning algorithm flow chart

Chapter 5 Experiment and Data Analysis

To evaluate the performance of the UWB localization system, the experiment was designed in this chapter. The four anchors were mounted on the vertex of the square area which can be seen in Fig. 2.18 with 4 m long and 3 m width, and three of them were lie on the ground while another was installed on the top surface of chair whose vertical distance to ground is 2.3 m. To construct Cartesian coordinate system, the anchor A_1 is the original point and the edge of A_1 and A_2 acts as x axis, while the y axis is the edge which is the projection to the ground between A_1 and A_4. The z axis is parallel to the height of A_4 from the bottom to top and goes through the original point.

The tag was connected to a data transmission module with serial port so it can send its position information to the host computer. Moreover, in order to keep the UWB ranging protocol more efficient to increase positioning accuracy and real-time ability, each UWB localization module transmit common messages rather than ranging messages via Zigbee modules, which is really mature and easy to use because there are no requirement to program the complicated protocol stack or build a multi-hop mesh network.

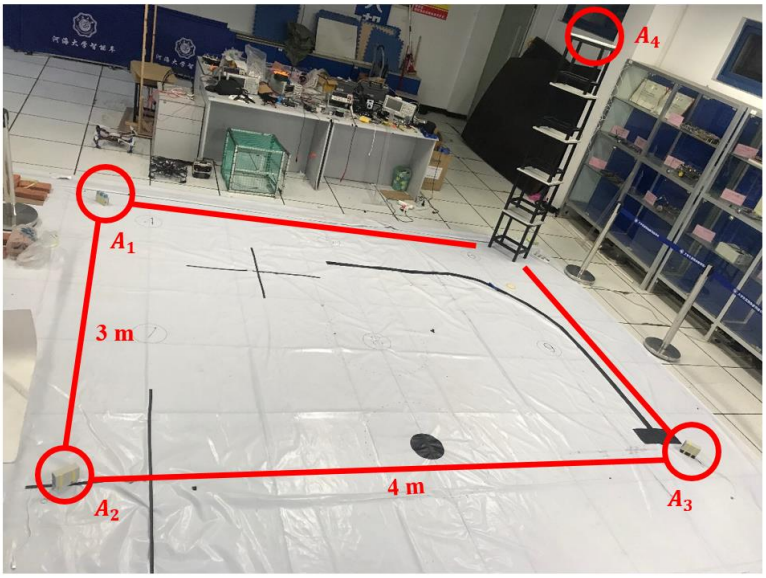

Fig. 2. 21 Photo of UWB localization experiment

This experiment can mainly divide to two aspect: with altimeter and without altimeter. The test environment is set in our laboratory and the static localization with a constant position was analyzed firstly. Then, the dynamic localization in the x, y axis and z axis scenarios were evaluated separately. In the x, y axis scenario three types of trajectory movement had been applied and recorded using rectangular, diagonal as well as triangle shape, as shown in Fig. 2.19.

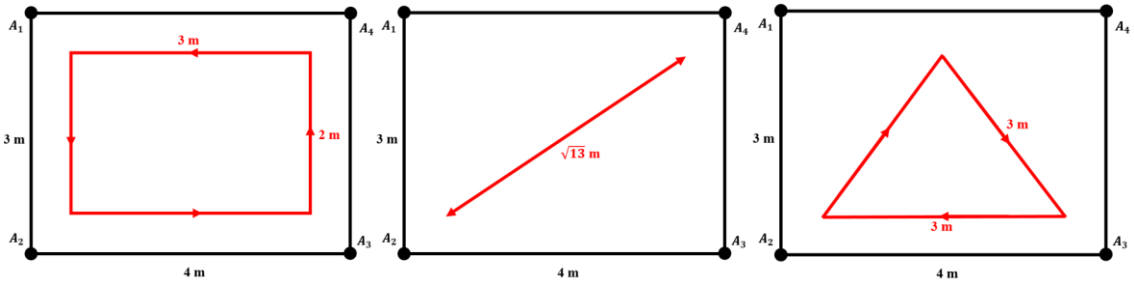

Fig. 2. 22 Three types of trajectory movement

Furthermore, the ranging data distribution graph based on time was also depicted in this case. However, since the limit of the evaluation tool, only a distribution graph established on time was performed in z axis scenario.

5.1 Positioning test without the altimeters

For the static situation, the tag was placed on the top surface of the chair. The ground-true position of it is $(1.5\ \text{m}, 2\ \text{m}, 0.6\ \text{m})$ and data analysis is drawn as below:

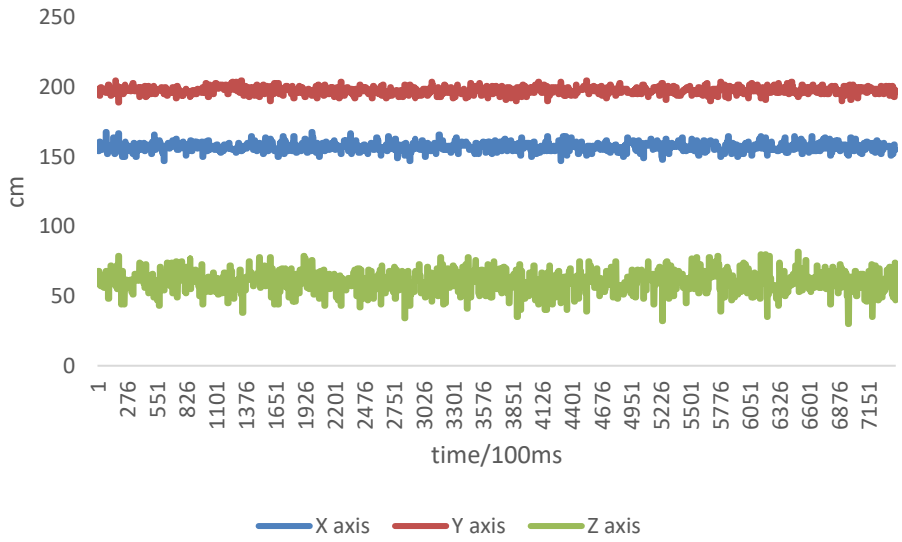

Fig. 2. 23 Ranging data distribution graph in static case

Table 1 Standard deviation in static case

Axis	Time phase	Standard deviation
X	1-7151	3.404
Y	1-7151	3.021
Z	1-7151	8.176

On the other hand, in the first scene of the dynamic situation the tag moved along the four rims of the red. The length of long side of the rectangular is 3 m and the width is 2 m. When moving on the red rectangular the tag was keeping constant height. Each of ranging data distribution graph about x, y axis is depicted below as well as their deviation was also analyzed. The second scene is a back and forth diagonal trajectory which was carried out and recorded similarly as well as the third scene about a regular triangle trajectory.

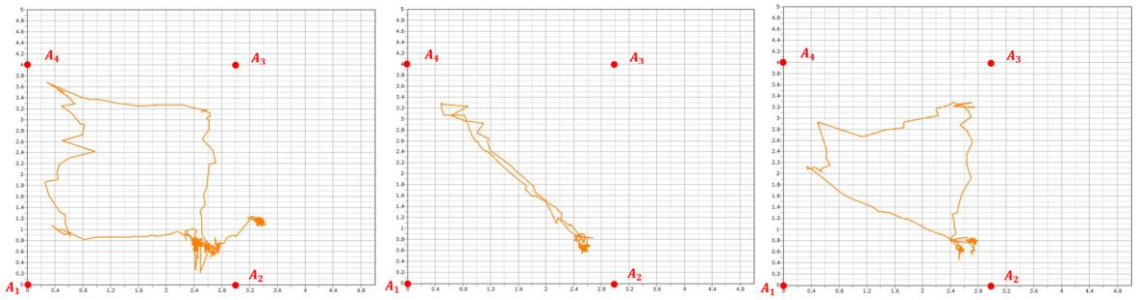

Fig. 2. 24 The trajectory of the rectangular, diagonal and triangular

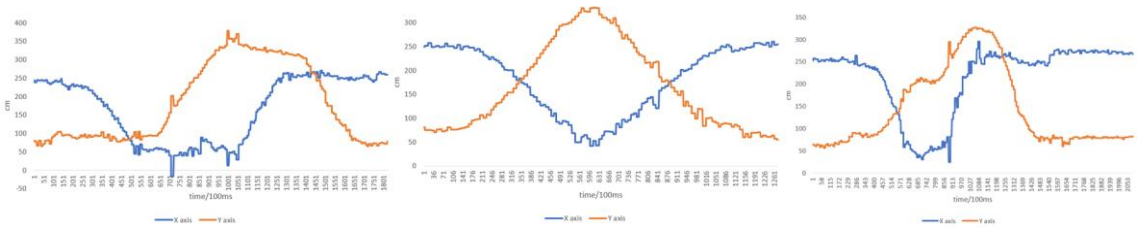

Fig. 2. 25 Ranging data distribution graph in x, y axis

In other respects, the evaluation of dynamic accuracy of z axis was executed here. The tag was mounted on the top surface of the chair with 0.6 m fixed height and moving randomly. Relevant data analysis is presented in Fig. 2.26 with 30.5 standard deviation. The result why the UWB localization system produce zero solution in this case may be because of the error of each UWB module, which also create a blind area above the ground plain.

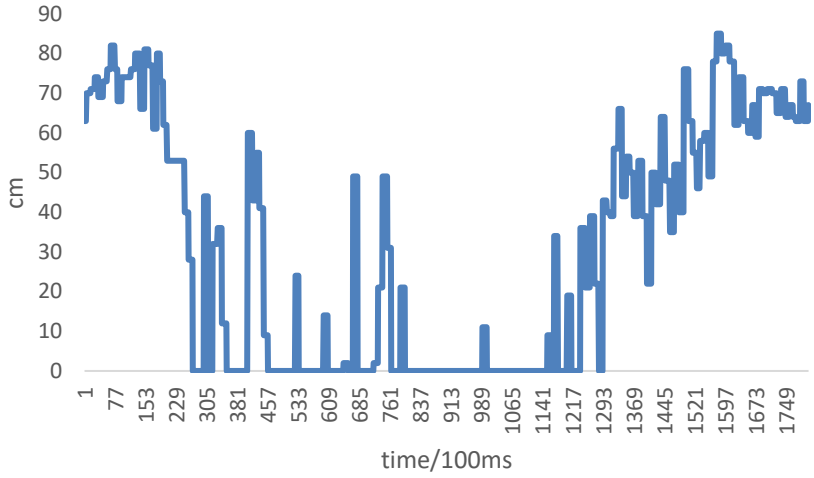

Fig. 2. 26 Ranging data distribution graph in z axis

5.2 Positioning test with the altimeters

In here those two scenarios (static and dynamic) is also discussed but the barometer was utilized to determine the position of z axis of each anchors. In the purpose of simplifying and minimizing the error of manual installation, the experiment data was recorded and shown as below:

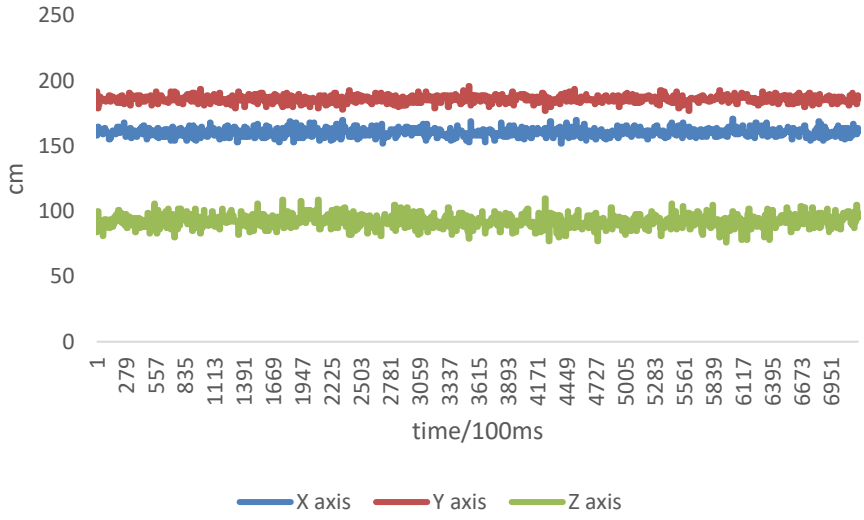

Fig. 2. 27 Ranging data distribution graph in static case

Table 2 Standard deviation in static case

Axis	Time phase	Standard deviation
X	1-6951	3.220
Y	1-6951	2.771
Z	1-6951	5.283

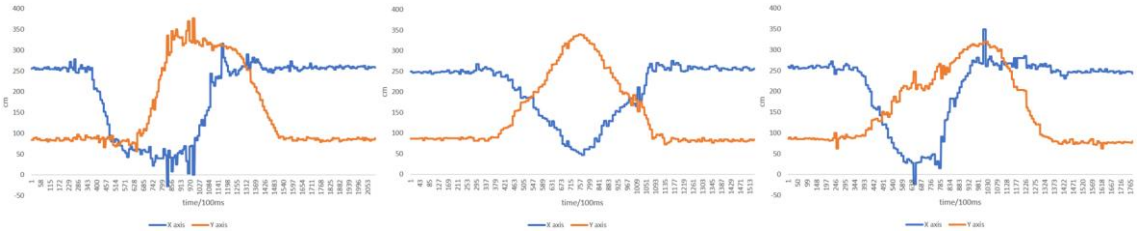

Fig. 2. 28 Ranging data distribution graph in x, y axis

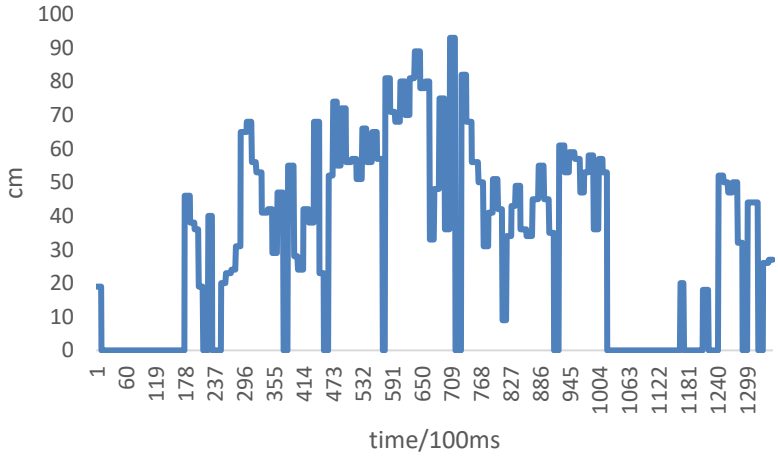

Fig. 2. 29 Ranging data distribution graph in z axis

By analyzing these ranging data, the standard deviation in static scenario was improved, but in dynamic scenario the magnitude of burr noise was increased. Moreover, the disaster in z axis of the dynamic situation does not get better.

Chapter 6 Conclusion

In this paper, an UWB localization system with altimeter was introduced. Though by using the barometer to calculate the height of each of four anchors, which may simplify the procedure of installation of the base station and minimize the error caused by manual operation, the noise of ranging data is enlarged by the noise of the barometer. Therefore, the proposed method cannot be utilized in real environment.

In order to optimize the performance of the UWB localization system, there are still a lot of improvement needed to be research, such as more advanced algorithm, multiple sensors fusion and so on, and more experiments need to be carry out.

References

[1] Sahinoglu, Zafer. *Ultra-wideband positioning systems*. Cambridge university press, 2008.

[2] Chen, Cheng, et al. "Low cost IMU based indoor mobile robot navigation with the assist of odometry and Wi-Fi using dynamic constraints." Proceedings of the 2012 IEEE/ION Position, Location and Navigation Symposium. IEEE, 2012.

[3] Liu, Xiaohan, Hideo Makino, and Kenichi Mase. "Improved indoor location estimation using fluorescent light communication system with a nine-channel receiver." IEICE transactions on communications 93.11 (2010): 2936-2944.

[4] Qiu, Chen, and Matt W. Mutka. "Silent whistle: Effective indoor positioning with assistance from acoustic sensing on smartphones." A World of Wireless, Mobile and Multimedia Networks (WoWMoM), 2017 IEEE 18th International Symposium on. IEEE, 2017.

[5] Tiemann, Janis, Florian Schweikowski, and Christian Wietfeld. "Design of an UWB indoor-positioning system for UAV navigation in GNSS-denied environments." Indoor Positioning and Indoor Navigation (IPIN), 2015 International Conference on. IEEE, 2015.

[6] Shi, Zhiyuan, et al. "A Nano-Quadcopter Formation Flight System Based on UWB Indoor Positioning Technology." 2018 13th International Conference on Computer Science ‘ Education (ICCSE). IEEE, 2018.

[7] Decawave DW1000 Product Brief. [Online]. Available: www.decawave.com

[8] Decawave DWM1000 Product Information: [Online]. Available: www.decawave.com

[9] Federal Communications Commission, *First Report and Order 02-48*, Feb. 2002.

[10] Jacob, Daniel J. Introduction to atmospheric chemistry. Princeton University Press, 1999.

[11] Cavcar, Mustafa. "The international standard atmosphere (isa)." *Anadolu University, Turkey* 30 (2000): 9.

[12] Li, Binghao, Bruce Harvey, and Thomas Gallagher. "Using barometers to determine the height for indoor positioning." *International Conference on Indoor Positioning and Indoor Navigation*. IEEE, 2013.

[13] Liu, Guangwen, et al. "Beyond horizontal location context: measuring elevation using smartphone's barometer." *Proceedings of the 2014 ACM International Joint Conference on Pervasive and Ubiquitous Computing: Adjunct Publication*. ACM, 2014.

[14] STMicroelectronics web site. [Online]. Available: www.st.com

[15] Decawave DW1000 hardware design guide. [Online]. Available: www.decawave.com